International Journal of Applied Mechanics
Vol. 9, No. 6 (2017) 1750084 (16 pages)

DOI: 10.1142/S1758825117500843

Finite Element Modeling and Experimental Studies of Stack-Type Piezoelectric Energy Harvester

L. V. Duong[*,**,‡‡], M. T. Pham[†], V. A. Chebanenko[‡], A. N. Solovyev[§,¶] and Chuong V. Nguyen[‖,††,‡‡]

[*]*Department of Mechanical Engineering and Energy in Transportation*
Le Quy Don Technical University, Ha Noi, Vietnam

[†]*Department of Engineering Mechanics and Automation*
Vietnam National University, Ha Noi, Vietnam

[‡]*Department of Vorovich Mechanics*
and Applied Mathematics Research Institute
Southern Federal University, Rostov on Don, Russia

[§]*Department of Theoretical and Applied Mechanics*
Don State Technical University, Rostov on Don, Russia

[¶]*Department of Mathematics, Mechanics and Computer Sciences*
Southern Federal University, Rostov on Don, Russia

[‖]*Institute of Research and Development, Duy Tan University*
Da Nang, Vietnam
[**]*leduong145@gmail.com*
[††]*chuongnguyen11@gmail.com*

Received 1 April 2017
Revised 17 July 2017
Accepted 22 July 2017
Published 22 September 2017

In this paper, closed-form coupled electromechanical one-dimensional (1D) model and finite element (FE) model for stack-type piezoelectric energy harvester (PEH) and delivery to a resistive load available in the literature were proposed. We obtained the values of some parameters of 1D model and set the boundaries of its applicability based on the comparison of the resonance frequency and output voltage between the FE model and 1D model. The numerical modeling results of the full-scale experiment with low-frequency pulse excitation of the stack-type PEH for the energy storage device are described. PEH is a multilayer axisymmetric piezoceramic package. The dependence between the output voltage and the current load rate under the harmonic and non-stationary mechanical action of the PEH is studied. The experimental results-to-numerical calculation correlation has shown their good coincidence, which allows using the analyzed numerical models to optimize the PEH design at the given external action frequency and the active resistance value of the external electric circuit. Besides, it found that the frequency dependence of the output voltage of the stack-type PEH is of a complex nature depending

[‡‡]Corresponding authors.

both on the compressive pulse loading level and the piezoelectric modulus value of the PEH sensitive element, and on the electrical load resistance.

Keywords: Finite element (FE); piezoelectric energy harvester (PEH); 1D model; approximate effective mass; stack-type; resonant frequency.

1. Introduction

Harvesting energy is an attractive alternative to battery-operated systems, especially for long-term, low-power consuming and self-sustaining electronic systems. In comparison with other conversion methods, piezoelectric energy harvesters (PEHs) have many advantages. For example, PEHs consist of piezoelectric ceramics, and electrodes which cover them. Therefore, PEHs can be made on the scale of microelectromechanical systems due to its simplicity. In addition, unlike the power generation methods that rely on heat conversion, a PEH presents no problems, such as heat isolation. PEH consists of two parts, namely mechanical and electrical. The mechanical part includes vibration was receiving structure and transducer. This part is subjected to dynamical loading and converts mechanical energy into electrical one. In turn, the electrical part rectifies energy and transfers it to storage and electric load. The PEHs have been intensively studied in the literatures where various PEHs were connected to a single load resistor [Chen *et al.*, 2016; Solovyev and Duong, 2016], as a simplified and usual view in considering a linear circuit is to replace the extraction circuit by its equivalent linear input resistance [Solovyev and Duong, 2016]. The power output has been optimized [Gatti, 2013; Solovyev and Duong, 2016] and has been normalized in dimensionless forms [Gatti, 2013; Zhang *et al.*, 2013b].

Piezoelectric transducers have two practical coupling modes, namely d_{33} and d_{31}. In d_{33} mode a force is applied in the direction of polarization and in d_{31} mode a force is applied in the perpendicular direction. Hence, PEHs can be divided into two types: axial type PEHs (d_{33} mode) and cantilever type PEHs (d_{31} mode) [Li *et al.*, 2014]. The cantilever type PEH was proved to be more appropriate for small force and low vibration level, at the same time the axial type is suitable for high force excitation [Anton and Sodano, 2007]. The cantilever type PEHs have received the most attention in the research studies in macro-scale as well as in micro-scale [Zaman *et al.*, 2010; Xu and Shengping, 2013; Zhang *et al.*, 2013c; Abas *et al.*, 2015; Li and Luo, 2017]. The axial type PEH is a single bulk of piezoceramic or a stack of piezoelectric layers attached one to each other and connected in parallel [Ali and Adhikari, 2013; Zhang *et al.*, 2013b].

The prospect for PEHs has also been analyzed by Ali and Adhikari [2013] by using a vibration absorber. In their work, a vibration absorber supplemented with a piezoelectric stack for both vibration confinement and energy harvesting. Moreover, from a circular cylinder Mehmood *et al.* [2013] systematically studied the concept of harvesting energy. Using piezo-shaped memory alloy composite, Namli and Taya [2011] also investigated a thermal energy harvester. They showed that the effect

of piezoelectrics and shape memory alloy is the main factor of the piezo-shaped memory alloy composite. Noted that the piezoelectrics and shape memory alloy are connected in series and subjected to fluctuating temperature. The resonance phenomenon has been analyzed by Boisseau *et al.* [2013]. It is shown that the output power of the vibration energy harvesters increases by using nonlinear springs. The influence on the plate's overall properties resulted from the surface elasticity and piezoelectricity of piezoelectric bimorph nano-actuators is modeled by a spring force exerting on the boundary of the bulk core [Zhang *et al.*, 2013a]. Recently, a finite element (FE) modeling for static and dynamic analyses of functionally graded piezoelectric beams has been developed by Lezgy-Nazargah *et al.* [2013]. Whereas, Chen *et al.* [2016] proposed a new strategy of electric power supply for highways. It can be used as a useful guideline for designing mechanical energy-harvesting systems in various road pavements.

Priya and Inman [2009] and Erturk and Inman [2011] developed many applications of piezoelectric energy harvesting (PEH). However, the development of theoretical models to predict the electromechanical response is equally important. The majority of the models have been based on a single-degree-of-freedom (SDOF) spring mass [Dutoit *et al.*, 2005; Twiefel *et al.*, 2008]. The use of such systems is a convenient model approach since it allows obtaining relationships between the output parameters of PEH (potential, power, etc.) and electrical, mechanical characteristics and resistance of the external electric circuit. By using the derived 2D equations, Zhang *et al.* [2013c] theoretically studied the model of antiparallel piezoelectric bimorph nano-actuators with surface effects. Using the commercially available software package ANSYS by FE analysis, Solovyev and Duong [2016] presented a detailed calculation of PEH having a form of a bimorph-circular plate, the contour of which in the device frame. Interestingly, based on Timoshenko theory an analytical method has been presented by Zhou *et al.* [2017] to obtain the in-plane static closed-form general solutions.

All the referred articles inform not only of the investigation in the field of different kinds of harvesters, but only of harvesters with passive load, cyclic loading regime. Unfortunately, a detailed data of these PEH results has not been given. Choosing the pulse loading regime is due to application field of stack-type PEH as a promising independent energy source, transforming the mechanical energy of periodic effects from an external environment. In particular, these stack-type PEH can be used for mechanical energy transform of the vibrations of rails of a railway transportation or roadway of the highway into electrical energy. Due to a high force excitation, the minimum value of stack-type PEH cross-section area is constrained by the strength of piezoelectric ceramics. Significant decrease of cyclic fatigue properties of poled piezo ceramics, which experience the mechanical loading combined with an electric field [Weitzinga *et al.*, 1999] is highlighted in many works [Weitzinga *et al.*, 1999; Lee *et al.*, 2003; Zhang *et al.*, 2003]. Basing on the above stated, such combined electromechanical action can decrease admissible cyclic

stresses twice [Zhang *et al.*, 2003]. The above is a brief analysis of the known works have shown that the problem of development a high power stack-type PEH with efficient output parameters under the action of pulsed loads is not yet resolved, although quite relevant.

In this paper, the FE method is employed to obtain the values of some parameters and set the boundaries of applicability of the 1D model consisting of a piezoceramic stack harvesting device and a resistive load [Dutoit *et al.*, 2005] based on comparison of the resonance frequency and output voltage between the FE model and theoretical model. The authors anticipate that these energy harvesting devices can be modeled accurately using the parameters proposed. An experimental rig has been set up to observe the response of the multilayer piezoelectric stack in the harvester. The authors have obtained the experimental and numerical results of the studies of time dependencies of the output characteristics of the multilayer PEH of axial type on the value of pulse mechanical compressive stress at different values of the electrical load resistance. Comparisons of the experimental results with the FE model are very successful and prove the validity of the FE model.

2. Theoretical Studies on the Applicability of the 1D Electromechanical Model by FE Analysis for the Stack-Type PEH

2.1. *Model of power harvesting system*

We consider stack-type PEH device as shown in Fig. 1. Energy is harvested through base excitations and the piezoceramic is operated in the {33} direction. We have considered two types of harvesters, namely without and with the boundary conditions on the side surface (conditions smooth contact), as shown in Figs. 1(a) and 1(b), respectively.

The first harvester, sketched in Fig. 1(a), is a piezoceramic harvester developed in [Dutoit *et al.*, 2005]. The model consists of an electrode piezoelectric element

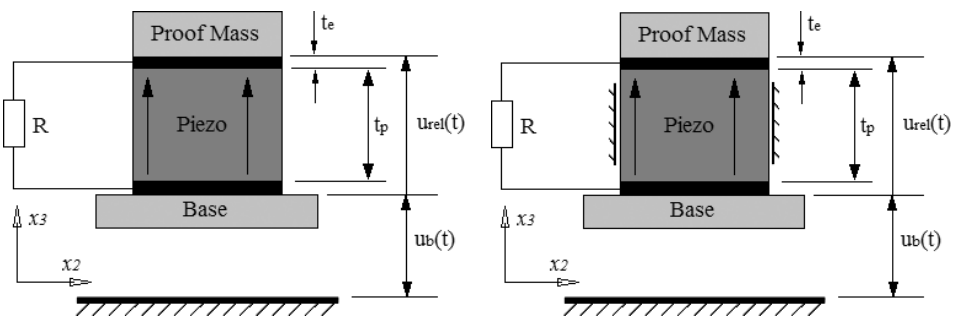

Fig. 1. Schematic diagrams of PEHs with two different boundary conditions: (a) First harvester; (b) Second harvester.

excited by a base input displacement, $u_b(t)$. The piezoelectric element has a height h_p, surface area A_p and is connected to a power-harvesting circuit, modeled simply as a resistor R. A proof mass, M_m, is also considered. Electrode thicknesses are taken to zero (i.e., ignored) in the analysis.

In Fig. 1, $u_b(t)$ is the harmonic base displacement

$$u_b(t) = u_0 e^{-i(2\pi f)t}, \tag{1}$$

where $u_0 = 0.1$ mm is the amplitude oscillation and f is the oscillation frequency.

Piezoelectric ceramic PZT-5H was used. Steel is used as the material of the proof mass. Thus, it can easily realize low resonant frequency corresponding to most vibration sources in our living environment as well as the vibration frequency. Geometrical parameters and material properties of the PEHs are listed in Table 1.

2.2. 1*D electromechanical model*

Dutoit *et al.* [2005] developed a closed-form coupled electromechanical 1D model of piezoelectric vibrational energy harvesting (Fig. 1).

From a force equilibrium analysis, the governing equations can be found in terms of the device parameters defined in Fig. 1:

$$\frac{d^2u_{\text{rel}}}{dt^2} + 2\xi_m\omega_n\frac{du_{\text{rel}}}{dt} + \omega_n^2 u_{\text{rel}} - \omega_n^2 d_{33} v = -k_1\frac{d^2u_b}{dt^2}; \tag{2}$$

$$R_{\text{eq}}C_p\frac{dv}{dt} + v + m_{\text{eq}}R_{\text{eq}}d_{33}\omega_n^2\frac{du_{\text{rel}}}{dt} = 0; \tag{3}$$

Equation (2) is simply Newton's equation of motion for a SDOF system and Eq. (3) is obtained from the electrical circuit. Where u_b is displacement of base, u_{rel} is a relative displacement of the proof mass, ξ_m is the mechanical damping ratio, $C_p = \varepsilon_{33}A_p/h_p$ is the capacitance, d_{33} is a piezoelectric constant, v is an output

Table 1. Geometrical parameters of the model and materials properties.[a]

									Sample 1	Sample 2	Sample 3
PZT surface area, A_p (mm^2)									100	100	150
Proof mass, M_m (g)									10	5	10
Material properties (PZT-5H)											
Density (kg/m^3)	c_{11}^E (GPa)	c_{12}^E (GPa)	c_{13}^E (GPa)	c_{33}^E (GPa)	c_{44}^E (GPa)	e_{31} (C/m^2)	e_{33} (C/m^2)	e_{15} (C/m^2)	$\varepsilon_{31}/\varepsilon_0$	$\varepsilon_{33}/\varepsilon_0$	
7500	126	55	53	117	35.5	−6.5	23.3	17	1710	1470	
Material properties (Steel)											
Density (kg/m^3)				Young's modulus (GPa)				Poisson's ratio			
7800				210				0.3			

Note: [a]$\varepsilon_0 = 8.85 \times 10^{-12}$C^2/Nm^2 is permittivity of free space, $\xi = 0.05$ is mechanical damping ratio.

voltage, k_1 is a correcting factor valid only for the first natural frequency. The equivalent resistance, R_{eq}, is the parallel resistance of the load and the leakage resistances, R and R_p, respectively. In general, the leakage resistance is much higher than the load resistance, so that $R_{\text{eq}} \approx R$.

The natural frequency of the harvester, ω_n, and the approximate effective mass are defined as

$$\omega_n = 2\pi f, \quad f_n = \frac{1}{2\pi}\sqrt{\frac{K}{M}}; \tag{4}$$

$$M = M_m + \frac{M_p}{n}; \tag{5}$$

where n is the coefficient of the approximate effective mass, n is equal to 3 [Dutoit *et al.*, 2005].

Solution of the Eqs. (2) and (3) is given in Eqs. (6)–(8), normalized by the base input acceleration:

$$\left|\frac{u_{\text{rel}}}{\ddot{u}_b}\right| = \frac{k_1/\omega_n^2\sqrt{1+(r\Omega)^2}}{\sqrt{\left[1-(1+2\xi_m r)\,\Omega^2\right]^2 + \left[(1+k_e^2)r\Omega + 2\xi_m\Omega - r\Omega^3\right]^2}}; \tag{6}$$

$$\left|\frac{v}{\ddot{u}_b}\right| = \frac{k_1 m_{\text{eff}} R_{\text{eq}} d_{33}\omega_n\Omega}{\sqrt{\left[1-(1+2\xi_m r)\,\Omega^2\right]^2 + \left[(1+k_e^2)r\Omega + 2\xi_m\Omega - r\Omega^3\right]^2}}; \tag{7}$$

$$\left|\frac{P}{(\ddot{u}_b)^2}\right| = \frac{\left(k_1^2 m_{\text{eff}}/\omega_n r k_e^2 R_{\text{eq}}\right) R\Omega^2}{\sqrt{\left[1-(1+2\xi_m r)\,\Omega^2\right]^2 + \left[(1+k_e^2)r\Omega + 2\xi_m\Omega - r\Omega^3\right]^2}}; \tag{8}$$

where $\Omega = \omega/\omega_n$ and $r = \omega_n RC_p$ are dimensionless parameters, P is the output power.

For a stack-type PEH device (Fig. 1), Eqs. (6)–(8) can be used to obtain the x_3-direction displacement responses, output voltage and output power of the harvester, respectively.

2.3. *Continual and finite element (FE) problem statements*

2.3.1. *Continual statement of problem of the electric elasticity*

In FE packages ANSYS the Rayleigh method is used, as a rule, to take account of the attenuation in composite, solid structures. We will now extend the Rayleigh method for taking account of attenuation, which has been described above, to structures containing elastic and piezoelectric media. In the case of piezoelectric media $\Omega_j = \Omega_{pk}$, we shall assume that the mechanical stress tensor $\boldsymbol{\sigma}$ and the electric induction vector $\mathbf{D}$ are related to the deformation tensor $\boldsymbol{\varepsilon}$ and the electric field strength vector $\mathbf{E}$ by the equations

$$\boldsymbol{\sigma} = \mathbf{c}_j^E \cdot\cdot(\boldsymbol{\varepsilon} + \beta_{dj}\dot{\boldsymbol{\varepsilon}}) - \mathbf{e}_j^T \cdot \mathbf{E}; \quad \mathbf{D} + \varsigma_d\dot{\mathbf{D}} = \mathbf{e}_j \cdot\cdot(\boldsymbol{\varepsilon} + \varsigma_d\dot{\boldsymbol{\varepsilon}}) + \mathfrak{e}_j^S \cdot \mathbf{E}, \tag{9}$$

where c_j^E are the components of the elastic constant tensor; e_j is piezoelectric stress coefficients; $\mathfrak{e}_j^S$ are the components of the dielectric permittivity tensor. (For elastic media $\Omega_j = \Omega_{ek}$ the piezomodules e_j are equal to zero.)

We shall assume that a piezoelectric device is a solid Ω consisting of N homogeneous domains $\Omega_j (j = 1, 2, \ldots, N)$, generally speaking, with different piezoelectric or elastic properties. We shall assume that, in the domains $\Omega_j = \Omega_{pk}$ with piezoelectric properties, the displacement vector $\mathbf{u}(x, t)$ and the electric potential $\phi(x, t)$ satisfy the system of equations ($\mathbf{f}_j$ is the mass force density vector)

$$\rho_j \ddot{\mathbf{u}} + \alpha_{dj} \rho_j \dot{\mathbf{u}} - \nabla \cdot \boldsymbol{\sigma} = \mathbf{f}_j; \quad \nabla \cdot \mathbf{D} = 0 \tag{10}$$

for the governing relations (9) and the formulae

$$\boldsymbol{\varepsilon} = (\nabla \mathbf{u} + \nabla \mathbf{u}^T)/2, \quad \mathbf{E} = -\nabla \phi, \tag{11}$$

where ρ_j is the continuous function of coordinates (density); α_{dj}, β_{dj}, ζ_d are the non-negative damping coefficients, and the other symbols are the standard designations for theory of electroelasticity with the exception of index "j", corresponding for area Ω_j.

For the media $\Omega_j = \Omega_{ek}$ with pure elastic properties, only stress fields would be considered. Similar Eqs. (9)–(11) and constitutive relationships are used with neglect electric fields and piezoelectrical connectivity effects. Equations (9)–(11) are added to the mechanical and electrical boundary conditions, as well as the initial conditions in the case of non-stationary problem.

In particular, for electrode (S_e), included in external circuit, besides a condition of constancy of the electric potential, which in this case is to be unknown function, it is added the condition defining electric current flowing through this electrode:

$$\int_{S_e} \dot{D}_n ds = I, \tag{12}$$

where I is the current of the circuit, which is in the case of free electrode, equals zero; D_n is the normal component of the vector of the electric induction.

2.3.2. *FE approach*

We use FE modeling in classic Lagrangian formulation to solve dynamic problems of acoustic electric elasticity. We choose coherent FE mesh specified in the areas Ω_{hj}, which approach area Ω_j. There are unknown field functions $\mathbf{u}$, ϕ and ψ in this mesh. We approximate them as

$$\mathbf{u}(\mathbf{x}, t) = \mathbf{N}_u^T(\mathbf{x}) \cdot \mathbf{U}(t), \quad \phi(\mathbf{x}, t) = \mathbf{N}_\phi^T \cdot \boldsymbol{\Phi}(t), \quad \psi(\mathbf{x}, t) = \mathbf{N}_\psi^T(\mathbf{x}) \cdot \boldsymbol{\Psi}(t), \tag{13}$$

where $\mathbf{N}_u$ is the shape function matrix for displacement field $\mathbf{u}$; $\mathbf{N}_\varphi$ and $\mathbf{N}_\psi$ are the shape vector-functions for the electric potential fields ϕ and speed potential in acoustic medium ψ, respectively; and $\mathbf{U}(t)$, $\boldsymbol{\Phi}(t)$, $\boldsymbol{\Psi}(t)$ are the global vectors of the corresponding nodal degrees of freedom.

FE modeling approximation (13) of the generalized formulations of dynamic problems (9)–(11), including principal and natural boundary conditions, results in the following system of differential equations:

$$\mathbf{M}\cdot\ddot{\mathbf{a}}+\mathbf{C}\cdot\dot{\mathbf{a}}+\mathbf{K}\cdot\mathbf{a}=\mathbf{F}. \tag{14}$$

$$\mathbf{M}=\begin{pmatrix}\mathbf{M}_{uu} & 0 & \tilde{\mathbf{R}}_{u\psi}\\ 0 & 0 & 0\\ \tilde{\mathbf{R}}^T_{u\psi} & 0 & -\mathbf{M}_{\psi\psi}\end{pmatrix},\quad \mathbf{C}=\begin{pmatrix}\mathbf{C}_{uu} & 0 & \mathbf{R}_{u\psi}\\ \varsigma_d\mathbf{K}^T_{u\phi} & 0 & 0\\ \mathbf{R}^T_{u\psi} & 0 & -\mathbf{C}_{\psi\psi}\end{pmatrix},$$
$$\mathbf{K}=\begin{pmatrix}\mathbf{K}_{uu} & \mathbf{K}_{u\phi} & 0\\ \mathbf{K}^T_{u\phi} & -\mathbf{K}_{\phi\phi} & 0\\ 0 & 0 & -\mathbf{K}_{\psi\psi}\end{pmatrix},\quad \mathbf{F}=\begin{Bmatrix}\mathbf{F}_u\\ \mathbf{F}_\phi+\varsigma_{\mathrm{d}}\dot{\mathbf{F}}_\phi\\ 0\end{Bmatrix}, \tag{15}$$

relatively of the vector of unknown $\mathbf{a}=[\mathbf{U},\mathbf{\Phi},\mathbf{\Psi}]^{\mathrm{T}}$. Here $\mathbf{C}_{uu}=\Sigma_j(\alpha_{dj}\mathbf{M}_{uuj}+\beta_{dj}\mathbf{K}_{uuj})$, where $\mathbf{M}_{uuj}$ and $\mathbf{K}_{uuj}$ are the structural FE of mass and stiffness matrix. Other elements of the submatrix (14), (15) are described in Belokon *et al.* [2002].

The FE modeling equation system for *eigenvalue* (*eigenfrequency*) problems has the following form:

$$-\omega^2\mathbf{M}\cdot a+\mathbf{K}\cdot a=0, \tag{16}$$

$$\mathbf{M}=\begin{pmatrix}\mathbf{M}_{uu} & 0\\ 0 & 0\end{pmatrix},\quad \mathbf{K}=\begin{pmatrix}\mathbf{K}_{uu} & \mathbf{K}_{u\phi}\\ \mathbf{K}^T_{u\phi} & -\mathbf{K}_{\phi\phi}\end{pmatrix}. \tag{17}$$

Steady-state vibration problems arise, when $\mathbf{F}_u=\tilde{\mathbf{F}}_u(\mathbf{x})\exp(j\omega t)$, $\mathbf{F}_\phi=\tilde{\mathbf{F}}_\phi(\mathbf{x})\exp(j\omega t)$, $\mathbf{a}=\tilde{\mathbf{a}}(\mathbf{x})\exp(j\omega t)$. It is easy to derive a system of linear algebraic equations from (14), (15) relatively of the amplitude vector $\tilde{\mathbf{a}}$ in the form:

$$\mathbf{K}_c\cdot\tilde{\mathbf{a}}=\tilde{\mathbf{F}}_c,\quad \tilde{\mathbf{F}}_c=\left[\tilde{\mathbf{F}}_u,\tilde{\mathbf{F}}_\phi,0\right]^T, \tag{18}$$

$$\mathbf{K}_c=\begin{pmatrix}\mathbf{K}_{uuc} & \mathbf{K}_{u\phi} & \mathbf{K}_{u\psi c}\\ \mathbf{K}^T_{u\phi} & -\mathbf{K}_{\phi\phi c} & 0\\ \mathbf{K}^T_{u\psi c} & 0 & -\mathbf{K}_{\psi\psi c}\end{pmatrix}, \tag{19}$$

$$\mathbf{K}_{\eta\eta c}=-\omega^2\mathbf{M}_{\eta\eta}+i\omega\mathbf{C}_{\eta\eta}+\mathbf{K}_{\eta\eta},\quad \eta=u,\psi, \tag{20}$$

$$\mathbf{K}_{u\psi c}=-\omega^2\tilde{\mathbf{R}}_{u\psi}+i\omega\mathbf{R}_{u\psi},\quad \mathbf{K}_{\phi\phi c}=\frac{1}{(1+i\omega\zeta_d)}\mathbf{K}_{\phi\phi}. \tag{21}$$

2.4. *Results and discussion*

The resonant frequency of the piezoelectric energy converter is one of the most important factors influencing the converting efficiency of a device from mechanical energy to electrical energy. It must be designed to match the environmental vibration frequency, which is the prerequisite to maximize the output power.

For 1D model, from Eq. (5), it is observed that resonant frequency of FEH is a function of coefficient of the approximate effective mass n. Coefficient n is equal to 3 as defined in [Dutoit *et al.*, 2005], however, in reality coefficient n depends on the geometric parameters and boundary conditions of the PEH. In this section, we investigate the dependence of the coefficient n on the geometric parameters and boundary conditions of the PEH.

Let us consider the impact on the resonant frequency of the height of the piezoelectric element h_p, surface area of the piezoelectric element A_p and proof mass M_m. The obtained dependences are shown in Fig. 2.

The coefficient n is determined from the condition of coincidence of the resonance frequency calculated using Eq. (4) and calculated by the FE model of the package ANSYS (Fig. 2). Figure 3 shows the relationship between the coefficient n and the height of the piezoelectric element h_p.

From Fig. 3, it is verified that the coefficient n decreases with increasing the proof mass M_m, and increases with increasing both the height of the piezoelectric element h_p and surface area of the piezoelectric element A_p.

Analysis of the results shows that the value of the coefficient n is not equal to a fixed value of 3 [Dutoit *et al.*, 2005]. The coefficient n varies depending on the geometric parameters and boundary conditions of the PEH. For the second harvester, a value $A_p = 1\,\text{cm}^2$ (this value was used in [Dutoit *et al.*, 2005]), the value of the coefficient n increases with the height of the piezoelectric element, and takes the value 2.7218 (≈ 3) at the height of the piezoelectric element $h_p = 20\,\text{mm}$. Thus, when using the 1D model to calculate the resonant frequency and output voltage/power of the harvester and note that the value of the coefficient n depends on the parameters of the harvester. The results from Fig. 3 allow to select the value of the coefficient n depending on the height h_p, surface area A_p of the piezoelectric element and proof mass M_m.

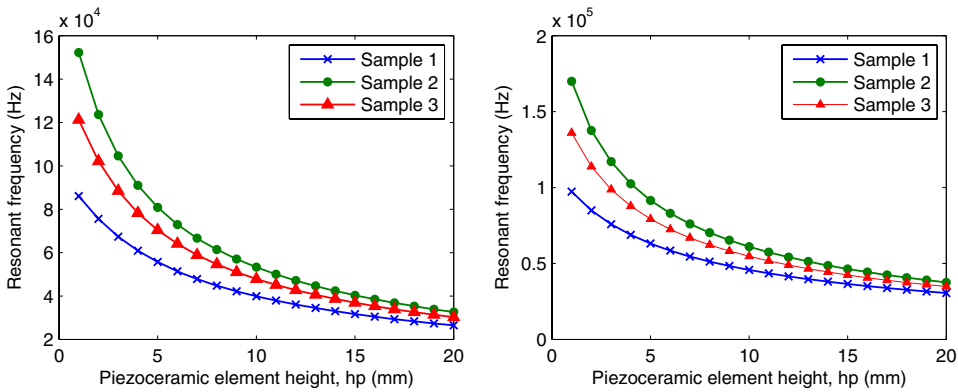

(a) (b)

Fig. 2. The dependence of the resonant frequency on the height of the piezoelectric element hp: (a) first harvester; (b) second harvester.

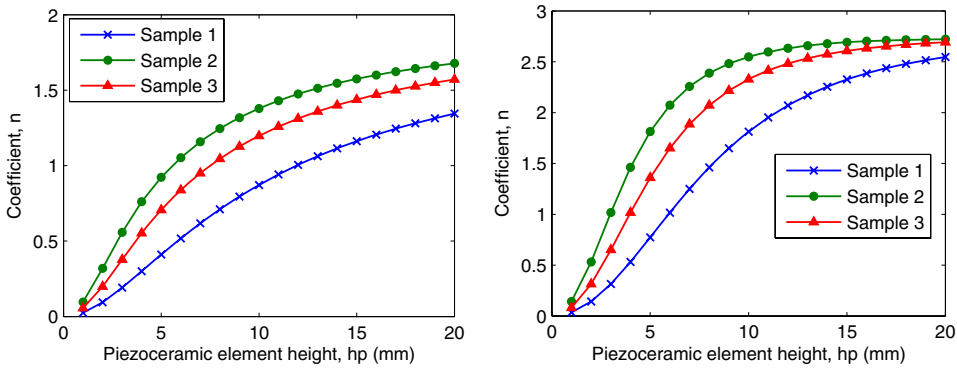

Fig. 3. The dependence of the coefficient n on the height of the piezoelectric element hp: (a) first harvester; (b) second harvester.

2.5. *Comparison of output potential*

Next, we consider the output voltage of PEH for the second harvester, depending on the oscillation frequency and load increases R.

In this section, the voltage outputs of PEH for the second harvester for frequencies between 10 kHz and 80 kHz were computed for five different electric loads (0.1, 1, 10, 100 and 1000 kOhm). With the value of the coefficient n is the value calculated above (Fig. 3), comparing the output voltage calculated using Eq. (7) (V_1) and calculated using the FE model (V_2), i.e., we study the influence of the geometric parameters and boundary conditions of the PEH on the coefficient $\lambda = V_1/V_2$. The results show that the values of the coefficient λ varies depending on the geometric parameters of the PEH and the load increases R. The results are presented in Table 2 with $M_m = 10\,\text{g}, A_p = 1\,\text{cm}^2$.

Figure 4 presents the dependencies of voltage on upper free electrode for five different electric loads on frequencies (between 10 kHz and 80 kHz) and height of the piezoelectric element $h_p = 10\,\text{mm}$ (Fig 4(a)), $h_p = 20\,\text{mm}$ (Fig. 4(b)), n and λ (Table 2).

The results show enough well coincidence, especially in the value range where the frequencies close to the resonant frequency.

Table 2. The values of the coefficient n and λ.

	R	0.1 kOhm	1 kOhm	10 kOhm	100 kOhm	1000 kOhm
$h_p = 10\,\text{mm}$	n	1.81	1.81	1.81	1.61	1.61
	λ	1	1	1	1.02	1.02
$h_p = 20\,\text{mm}$	n	2.73	2.73	2.73	2.68	2.68
	λ	1.12	1.12	1.12	1.18	1.18

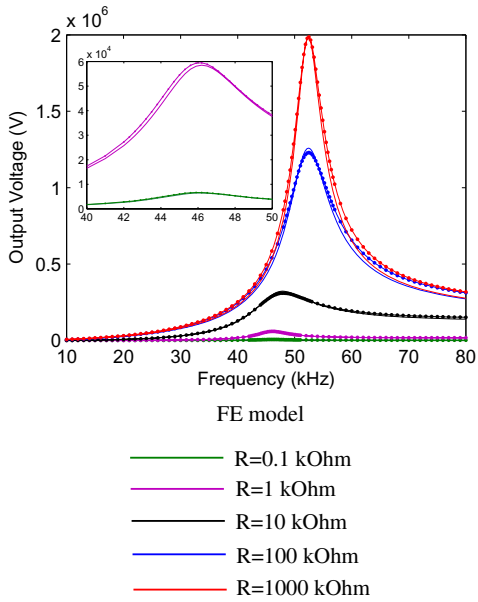

(a)

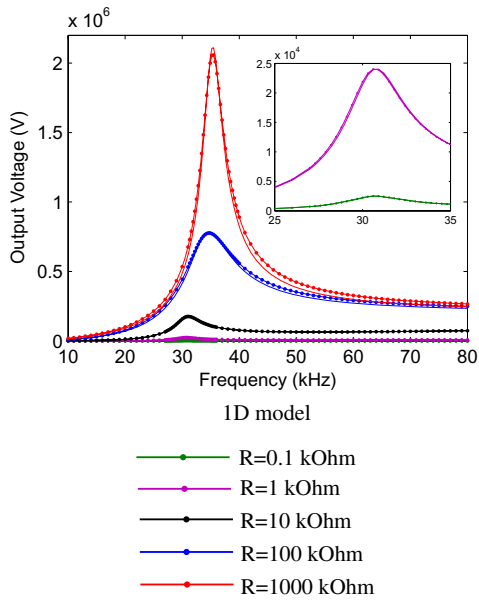

(b)

Fig. 4. Comparison between FE model (solid line) and 1D model (solid line with round dots) for the second harvester. In the plots: voltage computed across the resistor are 0.1, 1, 10, 100, 1000 kOhm, respectively.

3. Experimental Measurements Setup and Methodologies

The goal of this section is to experimentally verify the FE analytical in this paper for a multi-stack type PEH.

For carrying out of experimental researches, the multi-stack type PEH made from piezoceramics ЦТС-19 (analogue PZT-5A) with inner and outer diameters of 8 mm and 18 mm, respectively (piezoelectric constant $d_{33} = 360\,\text{pC/N}$). The multi-stack type PEH is composed of 11 piezoelectric layers of thickness $h = 1\,\text{mm}$ alternating with 0.1 μm thick pure silver internal electrodes (12 layers), as shown in Fig. 1(a). The multi-stack type PEH also has 3 mm thick passive layers (with no electrodes) at each end and with dimensions: inner diameter × outer diameter × thickness = 8 mm × 28 mm × 8.6 mm. The capacitance of the multi-stack type PEH is about 20.22 nF measured at 1 kHz without mechanical load.

The measurement setup is illustrated in Fig. 5. The diagram of the test setup is presented in Fig. 5(a). The pictures of the overall test setup frame and the detail of the test for the multi-stack type PEH are presented in Fig. 5(b). The energy harvesting experiments were carried out using a test unit consisting of (1) a frequency converter that specifies the frequency of the engine rotation from 10 to 1400 rev/min, (2) a Load Module — an engine with gear and eccentric disc and a rod, (3) a lever multiplier of the compressive force with conversion ratio of 50, (4) a multi-stack type PEH; (5) a strain-gauge dynamometer, (6) a support bracket of the multi-stack type PEH, (7) a strain amplifier, (8) an Analog to Digital Converter (ADC) and Digital to Analog Converter (DAC) (ADC/DAC), (9) a personal computer with installed PowerGraph, (10) a voltage divider (division factor to 1000), and a electrical resistance R.

The test stand creates a cyclic mechanical impact on the object under study with the help of the eccentric exciter. It carried an electric motor with gear-box and crank mechanism. The electric motor and gear-box are designed in single block. Gear-box is mounted vertically, and an eccentric disk is fixed to its axis. The crank mechanism converts the rotational motion into the translational motion of the connecting rod.

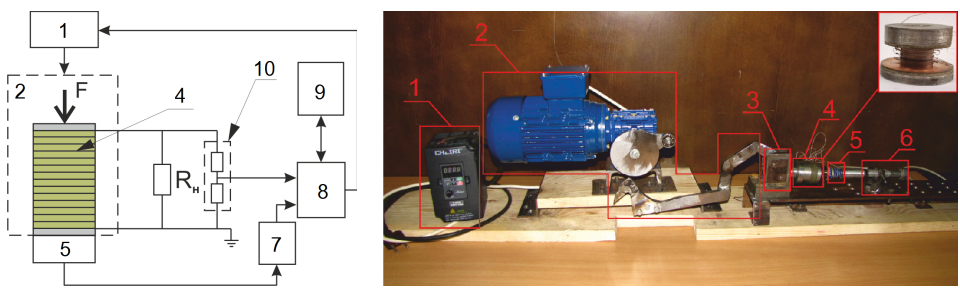

(a) (b)

Fig. 5. Energy harvesting characterization setup for multi-stack type PEH. (a) The diagram of the setup. (b) The overall picture of the test for the multi-stack type PEH.

We use a frequency converter ZVF11-H0004S2 to regulate the rotational frequency of the engine. For measuring electrical signals from the tensometer and multi-stack type PEH as well as for processing analog and digital information within the test bench used measuring voltage converter ADC/DAC and software E14-440 "Power-Graph". E14-440 provides a measurement of voltage DC and AC circuits in one or more measurement channels (maximum number of channels — 16 or 32, depending on the wiring diagram) using 14-bit ADC and multi-channel switch input channels. The operation of the voltage converter E14-440 performed from a personal computer through a standard interface USB 2.0.

The sample is under a mechanical cyclic loading of a compressive impulse force with an amplitude from 1 kN to 4 kN. For each cycle of compressive force measured by a dynamometer, registered time dependence of the value of compressive force and output voltage multi-stack type PEH at various discrete values of the load resistance R from 10 kohm to 22 Mohm. The time dependences of the characteristics of multi-stack type PEH was conducted with considering the influence of load resistance on the pulse shape of the output voltage of multi-stack type PEH. Such influence is characterized by the "degree of transmission non-distortion of an electrical signal", here, the piezoelectric response of sensitive element. The regime of undistorted transmission of an electrical impulse to the signal recorder is determined by the ratio.

The FE modeling equation system for *eigenvalue* (*eigenfrequency*) problems has the following form:

$$RC \geq \tau, \tag{22}$$

where τ — the pulse duration of the compressive force; R — the resistance of electrical load; and C — electric capacitance of the active element of PEH.

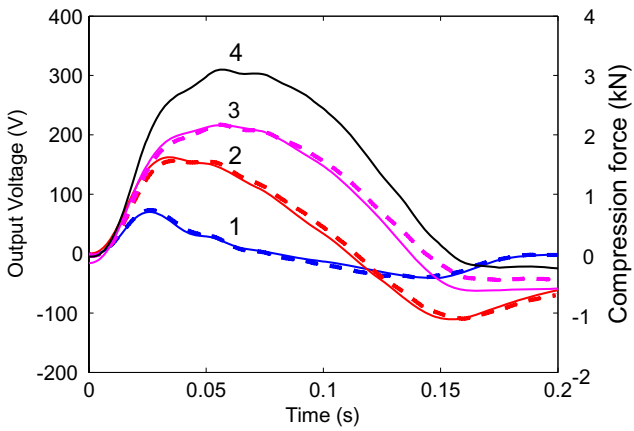

Fig. 6. (Color online) Comparison between experimental results (solid line) and FE model (dashed line) for multi-stack type PEH. In the plots: voltage measured across the resistors are 374 kOhm (blue — 1), 2572 kOhm (red — 2), 22770 kOhm (pink — 3), with the impulse of compressive force 3 kN applied at the upper surface of the multi-stack type PEH (black solid line — 4).

With the impulse of an external force (compressive force) 3 kN applied at the upper surface of the multi-stack type PEH from time 0 to 0.2 s, the experimental measurements are repeated for three different values of load resistance: 374, 2572 and 22770 kohm. The results of calculation in the package ANSYS and experimental data for the output voltage of the multi-stack type PEH, after 1 cycle load (in the time interval from 0 to 0.2 s) are shown in Fig. 6. In this case, ANSYS software is used to solve the problem based on the Newmark algorithm with the time step is 0.001 s. The maximum voltage output is about 70 volts for resistive load at 374 kohm, it is about 162 volts for resistive load at 2572 kohm and it is about 216 volts for resistive load at 22770 kohm.

According to Fig. 6, for all three resistive loads, the FE model yields a good match with the experimental data in terms of the generated voltage.

4. Conclusions

In conclusion, the FE method is employed to obtain the values of some parameters and set the boundaries of applicability of the 1D model consisting of a piezoceramic stack harvesting device and a resistive load available in the literature based on comparison of the resonance frequency and output voltage between the FE simulations and theoretical model. We also developed a method and a laboratory device for measurements of parameters of PEH a with mechanical impulse loading. It is established that the time dependence of the acting compressive mechanical impulse and the corresponding piezoelectric response at the output of PEH with different values of load resistance, the physical experiments and FE calculations show a fairly good agreement. Comparison forms of the piezoelectric response signals with increasing R and the pulses of the compression force showed that an increase in R — the forms of the output voltage tends to the form of the excitation pulse mechanical strain. It is established that the frequency dependence of the output voltage of axial type PEH has a complex character, that depends on both the level of compressive pulse loading and the value of the piezo-module d_{33} of the material sensitive element of the PEH and the electrical load resistance.

Acknowledgments

This work has been supported/partly supported by Vietnam National University, Hanoi (VNU), under Project No. QG.17.46.

References

Abas, Z., Yang, D. H., Kim, H. S., Kwak, M. K. and Kim, J. [2015] "Characterization of electro-active paper vibration sensor by impact testing and random excitation," *International Journal of Applied Mechanics* **7**(4), 1550065.

Ali, S. F. and Adhikari, S. [2013] "Energy harvesting dynamic vibration absorbers," *Journal of Applied Mechanics* **80**(4), 041004.

Anton, S. R. and Sodano, H. A. [2007] "A review of power harvesting using piezoelectric materials (2003–2006)," *Smart Materials and Structures* **16**, R1–21.

Belokon, A. V., Nasedkin, A. V. and Soloviev, A. N. [2002] "New schemes for the finite-element dynamic analysis of piezoelectric devices," *Journal of Applied Mathematics and Mechanics* **66**(3), 481–490.

Boisseau, S., Despesse, G. and Seddik, D. A. [2013] "Nonlinear H-shaped springs to improve efficiency of vibration energy harvesters," *Journal of Applied Mechanics* **80**(6), 061013.

Chen, Y., Zhang, H., Zhang, Y., Li, C., Yang, Q., Zheng, H. and Lü, C. [2016] "Mechanical energy harvesting from road pavements under vehicular load using embedded piezoelectric elements," *Journal of Applied Mechanics* **83**(8), 081001-1–081001-7.

Dutoit, N. E., Wardle, B. L. and Kim, S. G. [2005] "Design considerations for mems-scale piezoelectric mechanical vibration energy harvesters," *Integrated Ferroelectrics* **71**, 121–160.

Erturk, A. and Inman, D. J. [2011] *Piezoelectric Energy Harvesting* (John Wiley and Sons Ltd., New York).

Gatti, R. R. [2013] "Spatially varying multi degree of freedom electromagnetic energy harvesting," Ph.D. thesis, Curtin University, Australia.

Lee, K. L., Ai Kah Soh, A. K. and He, P. F. [2003] "Fatigue failure of ferroelectric ceramics subjected to cyclic inclined electric loading," *Scripta Materialia* **49**(9), 849–854.

Lezgy-Nazargah, M., Vidal, P. and Polit, O. [2013] "An efficient finite element model for static and dynamic analyses of functionally graded piezoelectric beams," *Composite and Structures* **104**, 71–84.

Li, H., Tian, C. and Daniel Deng, Z. [2014] "Energy harvesting from low frequency applications using piezoelectric materials," *Applied Physics Reviews* **1**, 041301.

Li, X. and Luo, Y. [2017] "Size-dependent postbuckling of piezoelectric microbeams based on a modified couple stress theory," *International Journal of Applied Mechanics* **9**(4), 1750053.

Mehmood, A., Abdelkefi, A., Hajj, M. R., Nayfeh, A. H., Akhtar, I. and Nuhait, A. O. [2013] "Piezoelectric energy harvesting from vortex-induced vibrations of circular cylinder," *Journal of Sound and Vibration* **332**(19), 4656–4667.

Namli, O. C. and Taya, M. [2011] "Design of Piezo-SMA composite for thermal energy harvester under fluctuating temperature," *Journal of Applied Mechanics* **78**(3), 031001.

Priya, S. and Inman, D. J. [2009] *Energy Harvesting Technologies* (Springer, New York).

Solovyev, A. N. and Duong, L. V. [2016] "Optimization for the harvesting structure of the piezoelectric bimorph energy harvesters circular plate by reduced order finite element analysis," *International Journal of Applied Mechanics* **8**(3), 1650029.

Twiefel, J., Richter, B., Sattel, T. and Wallaschek, J. [2008] "Power output estimation and experimental validation for piezoelectric energy harvesting systems," *Journal of Electroceramics* **20**, 203–208.

Weitzinga, H., Schneidera, G. A., Steffensa, J., Hammerb, M. and Hoffmann, M. J. [1999] "Cyclic fatigue due to electric loading in ferroelectric ceramics," *Journal of the European Ceramic Society* **19**(6–7), 1333–1337.

Xu, L. and Shengping, S. [2013] "Size-dependent piezoelectricity and elasticity due to the electric field-strain gradient coupling and strain gradient elasticity," *International Journal of Applied Mechanics* **5**(2), 1350015.

Zaman, M., Yan, Z. and Jiang, L. [2010] "Thermal effect on the bending behavior of curved functionally graded piezoelectric actuators," *International Journal of Applied Mechanics* **2**(4), 787–805.

Zhang, Y., Cheng, X. and Qian, R. [2003] "Fatigue behavior of ferroelectric ceramics under mechanically electrically coupled cyclic load," *Materials Science and Engineering A* **351**(1–2), 81–85.

Zhang, C., Zhang, C. and Chen, W. [2013a] "Modeling of piezoelectric bimorph nano-actuators with surface effects," *Journal of Applied Mechanics* **80**(6), 061015.

Zhang, H., Ye, G. and Zhang, Z. [2013b] "Acoustic radiation of a cylindrical piezoelectric power transformer," *Journal of Applied Mechanics* **80**(6), 061019-1–061019-5.

Zhang, C., Zhang, C. and Chen, W. [2013c] "Modeling of piezoelectric bimorph nano-actuators with surface effects," *Journal of Applied Mechanics* **80**(6), 061015-1–061015-7.

Zhou, Y., Nyberg, T., Xiong, G., Li, S., Zhou, H. and Bao, S. [2017] "Analytical solution of thick piezoelectric curved beams with variable curvature considering shearing deformation," *International Journal of Applied Mechanics* **9**(1), 1750006.